Reanalysis of $p + p$ reaction data: Probable absence of a ppK^- state

E. Epple* and L. Fabbietti†
Excellence Cluster "Origin and Structure of the Universe," 85748 Garching, Germany
and Physik Department E12, Technische Universität München, 85748 Garching, Germany
(Received 18 April 2015; published 15 October 2015)

In this work we question the hypothesis that the previously reported structure *X(2265)* in $p + p$ data is due to the kaonic nuclear bound state "ppK^-". We will show that it is rather unlikely that *X(2265)*, as reported by the DISTO collaboration, corresponds to a kaonic nuclear bound state. The main argument is based on the repetition of the DISTO analysis applied to a HADES data sample, which contains $p + p$ reactions at 3.5 GeV. We further discuss many aspects in connection with the $pK^+\Lambda$ final state and the $\Lambda(1405)$ resonance. The results point to possible problems in the interpretation of the DISTO data.

DOI: 10.1103/PhysRevC.92.044002 PACS number(s): 13.75.Jz, 13.75.Cs, 21.30.Fe, 21.45.−v

I. THE $pK^+\Lambda$ FINAL STATE IN $p + p$ REACTIONS

Since the first measurement of open strangeness production via the reaction

$$p + p \rightarrow p + K^+ + \Lambda \tag{1}$$

was reported [1], many experiments have exclusively measured this final state. Three issues were mainly investigated: the production of N^* resonances and their subsequent decay into $K^+\Lambda$ [2–10], the $p\Lambda$ final-state interaction [7,11–13], and the cusp structure appearing at 2.13 GeV in the $p\Lambda$ invariant mass distribution [14–16]. A fourth issue was recently added to this list with the investigation of the kaonic nuclear bound state $\overline{K}NN$ by the DISTO collaboration [17,18]. In this analysis the following scenario was investigated:

$$\begin{aligned} p + p \rightarrow\ & \text{"}ppK^-\text{"} + K^+ \\ & \hookrightarrow p + \Lambda. \end{aligned} \tag{2}$$

Here, a kaonic nuclear bound state $\overline{K}NN$, also called "ppK^-," is produced in $p + p$ reactions together with a K^+, and its nonmesonic decay in a $p\Lambda$ pair has been considered. This state is a bound state of an antikaon and two nucleons and is currently investigated in several experimental programs [19–22]; see also references in Ref. [10] for theoretical works in this field. The aim of this work is to cross-check the claim that the observed structure [named *X(2265)*, $M = 2267$ MeV/c^2 and $\Gamma = 118$ MeV] in the so-called deviation spectrum of Refs. [17,18] corresponds to the signature of an intermediate $\overline{K}NN$ cluster to the final state (1).

In the following, we explain what a deviation spectrum is, what difficulties arise from this method, and why the absence of *X(2265)* at lower beam energies is not linked to the absence of $\Lambda(1405)$ production, which is considered a doorway for the formation of $\overline{K}NN$ [23,24]. We further discuss whether a $\overline{K}NN$ production strength of 17% of the total $pK^+\Lambda$ production cross section at $E_{\mathrm{Kin}} = 2.85$ GeV, as reported in Ref. [25], is a realistic scenario, given the upper limits for *X(2265)* from Ref. [25] and from this work. The discussion is completed by summarizing all $p\Lambda$ mass spectra published so far, where no clear signature of *X(2265)* or any other kind of "ppK^-" signal is visible.

II. THE 2.5 GeV AND 2.85 GeV DISCREPANCY

After the publication of the DISTO results on the formation of a "ppK^-" in $p + p$ reactions at a beam kinetic energy of 2.85 GeV [17,18], the same authors also analyzed a data set measured by DISTO at a beam kinetic energy of 2.5 GeV [25]. Despite the expectation that as much as 33% of the observed yield of the structure *X(2265)* at 2.85 GeV should be visible also at the lower beam energy of 2.5 GeV, no signal appeared in the data. Therefore, an upper limit of $0.2\% \pm 2.1\%$ of the $pK^+\Lambda$ production cross section was estimated [25].

A. Depletion of $\Lambda(1405)$ yield

The missing signature of *X(2265)* at 2.5 GeV was explained by the lower abundance of the $\Lambda(1405)$ resonance at this energy which is, according to Refs. [23,24], a doorway for the formation of $\overline{K}NN$ in $p + p$ reactions [26]. The abundance of the $\Lambda(1405)$ resonance was, however, only roughly estimated on the basis of the missing mass distribution to the proton and K^+ (MM_{pK^+}) at 2.85 and 2.5 GeV. In this approach the high-mass region of the MM_{pK^+} spectra, which includes among others the contributions by $\Lambda(1405)$ and $\Sigma(1385)^0$, was considered and the $\Lambda(1405)$ production at 2.5 GeV was estimated to be maximally 10%, as for the data set at 2.85 GeV [25]. This estimation assumed that, first, the statistics in the resonance region of the MM_{pK^+} spectrum contain only the resonances $\Lambda(1405)$ and $\Sigma(1385)^0$ and, second, that the $\Sigma(1385)^0$-to-$\Lambda(1405)$ production ratio is the same for the two energies. The first assumption was disproved by the investigation of the $\Lambda(1405)$ resonance at a beam energy of 3.5 GeV [27]. Indeed, in the latter work the individual contributions to the MM_{pK^+} spectrum were determined and it was found that a substantial contribution stems from the production of $\Lambda(1520)pK^+$, $\Sigma^+\pi^-pK^+$, and $\Delta^{++}(1232)\Sigma^-K^+$ final states. While the $\Lambda(1520)$ production is below threshold at 2.5 GeV ($E_{\mathrm{kin}}(\mathrm{Threshold}) = 2.77$ GeV)

*eliane.epple@ph.tum.de
†laura.fabbietti@ph.tum.de

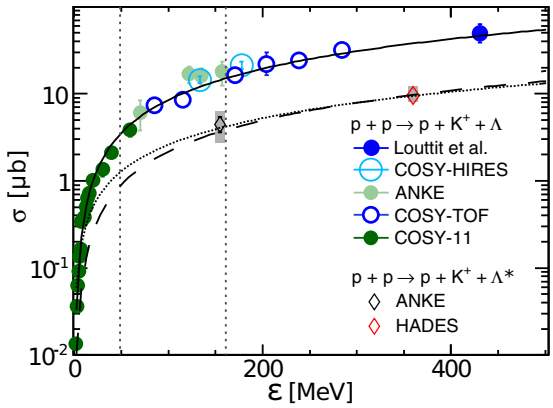

FIG. 1. (Color online) Compilation of measured $pK^+\Lambda$ (circles) and $pK^+\Lambda^*$ (diamonds) cross sections. The parametrization that describes the $pK^+\Lambda$ data is taken from Refs. [9,28]. The long dashed curve shows this parametrization scaled down to fit to the two $pK^+\Lambda^*$ data points and the dotted curve is a free fit of the Fäldt–Wilkin parametrization to the two points [27,29]. The vertical lines show the $pK^+\Lambda^*$ excess energy for the two DISTO data sets.

and probably small at 2.85 GeV, the other two final states will definitely contribute to the observed yield in the high-mass region of the MM_{pK^+} spectra, which was measured by DISTO. The second assumption about a constant $\Sigma(1385)^0$-to-$\Lambda(1405)$ production ratio is also questionable because the analysis in Ref. [30] showed that, at 3.5 GeV, this ratio is reduced by about 15% in comparison with the ratio measured by the ANKE collaboration at $E_{\mathrm{Kin}} = 2.83$ GeV [29]. Both values have, however, large uncertainties so that it is difficult to extrapolate to lower energies.

We suggest an alternative ansatz to compare the $\Lambda(1405)$ production cross section at the two DISTO energies. In Ref. [27] the energy dependence of the production cross section of the $pK^+\Lambda(1405)$ final state was determined on the basis of the values measured in $p + p$ collisions [27,29]. Figure 1 shows a compilation of measured cross sections from the $pK^+\Lambda$ and $pK^+\Lambda^*$ final states versus the excess energy. The two vertical dashed lines mark the excess energy for the $\Lambda(1405)$ production for the two data sets, measured by DISTO (48.8 and 161.2 MeV). The $pK^+\Lambda$ data are well described by a Fäldt–Wilkin parametrization, as done in Refs. [9,28]. By assuming a similar behavior of the two channels close to threshold, we scaled the $pK^+\Lambda$ curve down so that it fits the data points of the $pK^+\Lambda^*$ final state (long-dashed curve). We also performed a free fit of the mentioned parametrization from Refs. [9,28] to the two data points, which also describes them well (dotted curve). With help of the two curves the ratio of the Λ^* production cross section between the two DISTO energies was determined to be $\sigma_{pK^+\Lambda(1405)}(2.5\ \mathrm{GeV})/\sigma_{pK^+\Lambda(1405)}(2.85\ \mathrm{GeV}) = 0.23$, for the scaled curve and 0.3 for the curve based on the free fit to the data. The ratios show that the cross section of $\Lambda(1405)$ production at the 2.5 GeV data set is in any case a sizable fraction of that at 2.85 GeV. Following the assumption that the $\overline{K}NN$ production in $p + p$ collisions should proceed through the intermediate formation of a $\Lambda(1405)$, at least 23% of the observed *X(2265)* yield at 2.85 GeV should be expected at the lower energy.

In fact, the fraction of events affected by the $\Lambda(1405)p$ final-state interaction should be even higher at lower energies due to phase-space considerations [11]. Provided that the hypothesis of the $\Lambda(1405)$ being a doorway for the creation of "$\overline{p}pK^-$" is valid, that would result in an increased number of $\overline{K}NN$ per $\Lambda(1405)$.

Thus, we argue that the reasoning in Ref. [25] regarding the absence of a *X(2265)* signal at the 2.5 GeV DISTO data is not convincing because the $\Lambda(1405)$ yield at lower energies is larger than estimated by the authors.

B. Problem of deviation spectra

To provide a further cross-check of the results reported by the DISTO collaboration, we repeated the analysis of Refs. [17,18,25] and produced so-called deviation spectra. The original idea behind this approach was that any measured event distribution in a given observable which deviates from a purely phase-space-driven production process hints at the presence of a new signal. The deviation spectrum is obtained by dividing the experimental event distribution of an observable by the same simulated distribution obtained by employing phase-space simulations of the final state.

The data for this analysis [10,31–33] stem from the $p(E_{\mathrm{Kin}} = 3.5\ \mathrm{GeV}) + p$ reaction measured by the high-acceptance dielectron spectrometer (HADES) at the SIS18 synchrotron (GSI Helmholtzzentrum in Darmstadt, Germany). For details about the spectrometer and the experiment, see Refs. [10,34]. In the following discussion deviation spectra were obtained by dividing the measured event distribution of the invariant mass distribution of p-Λ pairs ($IM_{p\Lambda}$) by the corresponding simulated spectrum. The simulations were performed under the assumption that the three particles in the final state (1) are produced via phase space only. The division is performed with measured spectra which means that the data are shown inside of the HADES acceptance and are filtered by the event-selection procedure. Because the $pK^+\Lambda$ events were obtained within two different regions of the spectrometer acceptance (HADES and WALL; see Ref. [10] for details), we present two different deviation spectra in Figs. 2 and 3, respectively.

The two figures show several deviation spectra obtained under different data selections. While the red histograms show the deviation spectra for the full statistics as analyzed in Ref. [10], the long-dashed histogram represents the result after applying the very same cuts as done in the analysis by DISTO: $|\cos\theta_p| < 0.6$ and $-0.2 < \cos\theta_{K^+} < 0.4$ [17,18]. To point out the impact of such subsequent cuts, we further restricted the proton angle from 0.6 to $|\cos\theta_p| < 0.4$, while leaving the cut for the kaons unchanged; this is illustrated by the light-green histograms. A remarkable result (violet dotted in Fig. 2) is obtained if one only selects events where $M_{K^+\Lambda} > 1810\ \mathrm{MeV}/c^2$.

Before interpreting these spectra note that, first, it was shown already that phase-space production is not a suited model to describe the $pK^+\Lambda$ final state at a beam energy of 3.5 GeV [31,32], so we do not expect *a priori* to retrieve

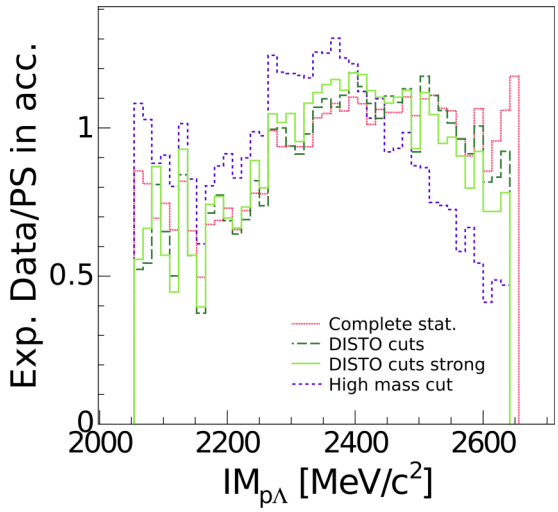

FIG. 2. (Color online) Different deviation spectra obtained by dividing the reconstructed $pK^+\Lambda$ events by phase-space simulations in the HADES acceptance.

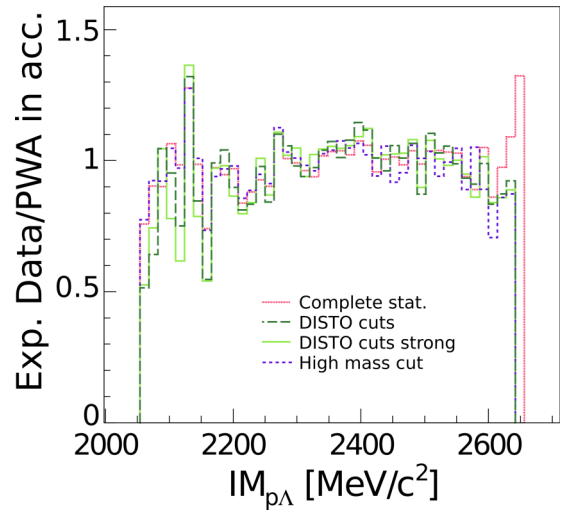

FIG. 4. (Color online) Different deviation spectra obtained by dividing the reconstructed $pK^+\Lambda$ statistics by a partial wave analysis model [10] in the HADES acceptance.

a flat deviation spectrum from this method and, second, most importantly, if the data are not described well by the simulation any further applied cut might have a different influence on the measured and the simulated spectra. This is the reason why the deviation spectra drastically change under different cut conditions. One can see, in particular for the HADES case, that the applied cuts start to deplete the deviation spectra from 2500 MeV/c^2 on. As a consequence, one obtains a deviation spectrum with a rising slope up to 2400 MeV/c^2 and a falloff for larger masses. This spectrum could be seen as broad peak structure, but it reflects only the effect of the kinematical cuts. Such an effect is also observed for the WALL data set in Fig. 3, where the green-dashed histogram shows a small structure at 2250 MeV/c^2.

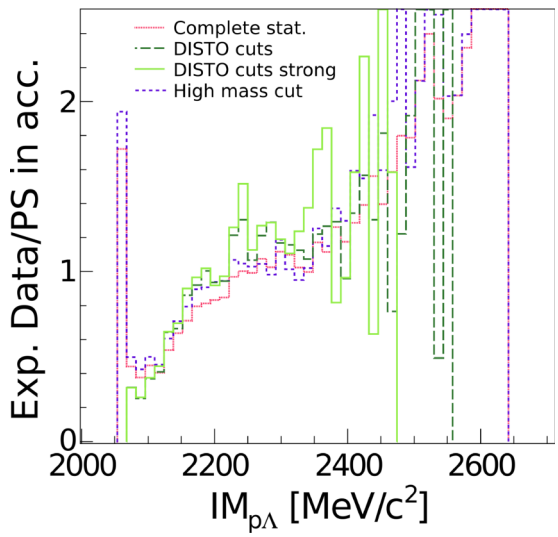

FIG. 3. (Color online) Different deviation spectra obtained by dividing the reconstructed $pK^+\Lambda$ events by phase-space simulations in the WALL acceptance.

In order to clarify these observations we want to present deviation spectra that we obtained by dividing the measured spectra by a partial wave analysis (PWA) model [35,36]. This model is based on a partial wave analysis of the measured $pK^+\Lambda$ data and contains only resonant (via the decay of heavy N^* resonances) and nonresonant $pK^+\Lambda$ production [10]. The model was compared to the measured events in many observables to gain confidence in the solidness of its data description. The deviation spectra in Fig. 4 are shown under the very same cut conditions as for the spectra with the phase-space simulations. In contrast to Figs. 2 and 3, the deviation spectra are in this case rather flat around one and the shape does not change when additional cuts are applied. This is entirely due to the correct description of the data by the PWA [10] so that the applied cuts, therefore, act symmetrically on the data and the model.

Summarizing, we have shown that deviation spectra strongly depend on the model to which the data are compared. If the simulation model is not fully adequate, the applied cuts may distort the deviation spectrum drastically and no reliable conclusions can be drawn. We thus consider this method as suboptimal to look for peak structures. From our perspective, thus, it is not astonishing that a certain structure at 2.85 GeV cannot be retrieved at 2.5 GeV in the DISTO data set.

III. DEVIATION SPECTRA REVISITED

We want to extend our discussion of deviation spectra to other energies. Indeed, the idea of comparing phase-space simulation to experimental data for the reaction (1) dates back to Ref. [37]. There, inclusive spectra of the missing mass to the kaon were divided by phase-space distributions at different kaon angles and beam kinetic energies. The result of Ref. [37] is shown in Fig. 5. The deviation spectrum differs from unity in the high-missing-mass region [the missing mass to the kaon (MM$_{K^+}$) corresponds to the mass of the residue X with which it is produced, e.g., $X = p\Lambda$ or $\Sigma N\pi$]. The horizontal gray

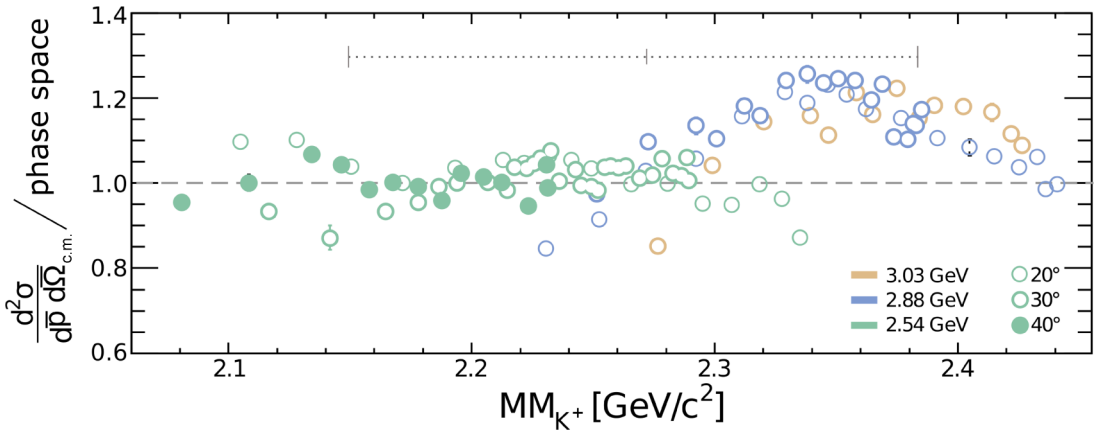

FIG. 5. (Color online) Spectra of the missing mass to the K^+, measured inclusively in $p + p$ reactions at three different beam kinetic energies [37]. The experimental spectra were divided by phase-space simulations. The gray horizontal bar indicates the range of the signal of *X(2265)*.

line indicates the signal range of *X(2265)*. No deviation at $MM_{K^+} = 2267$ MeV/c^2 is visible in these data sets. Indeed, the authors of Ref. [37] investigated the deviations in Fig. 5 under the assumption of a dibaryon being produced together with the kaon. However, they also considered the fact that the presence of N^* resonances in the data might cause the observed deviations from phase space, as was already suggested by an earlier work [2].

IV. ANY SIGNS OF A LARGE VISIBLE SIGNAL?

Since no *X(2265)* signal at the 2.5 GeV DISTO data has been found, an upper limit for its production strength of $0.2\% \pm 2.1\%$ of the total $pK^+\Lambda$ production cross section has been estimated [25]. An independent analysis of $p + p$ data measured by HADES has also set an upper limit on the production of a $\overline{K}NN$ in $p + p$ reactions at $E_{\mathrm{Kin}} = 3.5$ GeV [10]. The major difference between the DISTO and the HADES analysis is that, in the former case, visible bumps in the $p\Lambda$ invariant mass spectrum were associated with a signal whereas the latter analysis is done with help of a PWA [35,36]. In the PWA the amplitude strength of a wave associated with the production of a kaonic nuclear bound state was determined and coherently added to all other contributing waves. These two different approaches prevent, however, a direct comparison of the signal strength and the upper limits. In the best case, a partial wave analysis would be performed on the three data sets simultaneously. For the time being, we performed a simple incoherent analysis of the data to extract the upper limit of a *visible signal strength* in order to compare it consistently to the DISTO results. Such an extracted limit does not necessarily correspond to the real signal strength which is maximally compatible with the data because interferences with other signals are neglected in this approach.

A. An incoherent upper limit for the $\overline{K}NN$ production at 3.5 GeV

To carry out this analysis, we used the acceptance-corrected $p\Lambda$ invariant mass spectrum. The PWA solution from Ref. [10] delivers a model that describes the experimental spectrum well without including a $\overline{K}NN$ cluster signal. Although the PWA analysis was performed within the detector acceptance, an extrapolation of the solution to the full solid angle is possible. This way, with help of the 4π model, the measured data can be corrected to the full solid angle [33]. Figure 6 shows the reconstructed experimental data in 4π overlayed with the PWA solution. To extract an upper limit we added a Breit–Wigner signal with varying mass, width, and amplitude to the PWA solution (signal hypothesis) and compared the new spectra to the data. We consider the model compatible with the data, if the confidence level of the signal strength (CL_s [38–40]) is smaller than 95%. Since there are small uncertainties from the acceptance correction (gray error bars in Fig. 6), the upper limit was determined four times. Each time the signal hypothesis was compared to the experimental data which were corrected with one of the four best PWA models of Ref. [10].

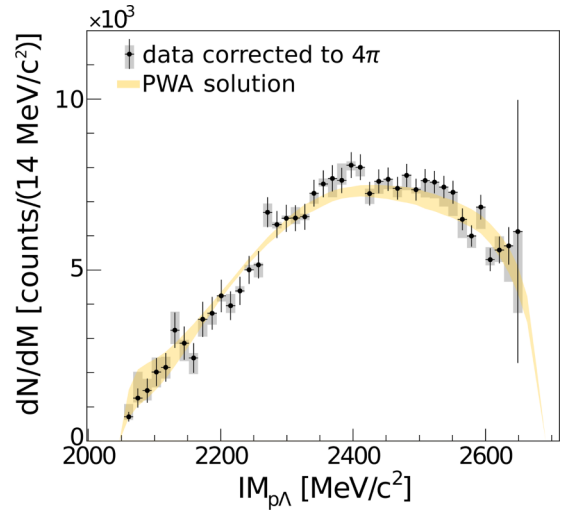

FIG. 6. (Color online) Acceptance- and efficiency-corrected $p\Lambda$ invariant mass distribution in 4π [33]. The yellow band shows the 4π solutions from the PWA analysis without the inclusion of a kaonic nuclear cluster [10].

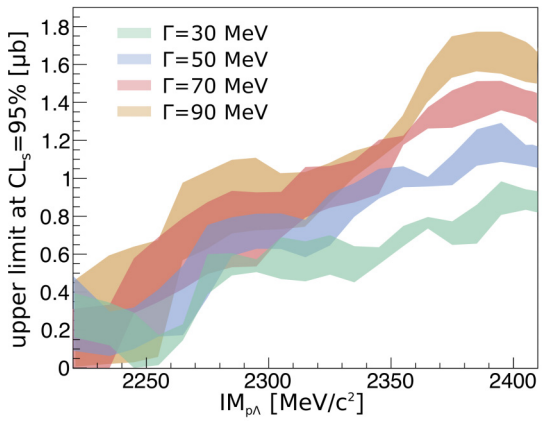

FIG. 7. (Color online) The incoherent upper limit as a function of the $\overline{K}NN$ mass for four different widths of the bound state. The spread of the limit (widths of the bands) comes from the different results which are obtained from the four best solutions of the PWA [10].

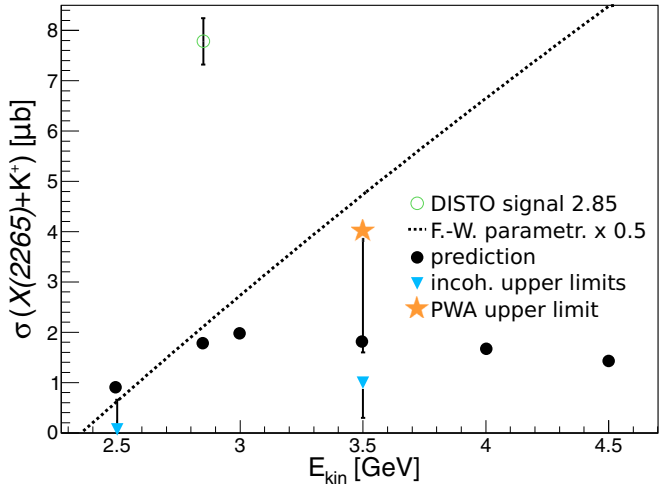

FIG. 8. (Color online) Predicted cross sections of a kaonic nuclear cluster production from Ref. [41] (filled circles). The signal strength of the DISTO observation (open circle) and the upper limits from DISTO and HADES (triangle) given for the properties of *X(2265)*. The coherent upper limit from a PWA analysis [10] (star) is given at the *X(2265)* mass but for a width of 70 MeV. Also shown is the Fäldt–Wilkin parametrization of the $\Lambda(1405)$ cross section from Fig. 1 (dotted).

The resulting upper limit, as a function of the mass of the bound state, is shown in Fig. 7 for four different signal widths (30, 50, 70, and 90 MeV/c^2). The width of the curves is due to the different upper limits obtained with the four different PWA models. The upper limit of about 0.7 μb (in the relevant mass range) is below the coherent upper limit of the PWA of Ref. [10], which is consequential because the interferences included in the PWA may hide the signal which makes it possible to include more signal strength while the spectra stay smooth.

We also determined an upper limit specifically for the *X(2265)* properties ($M = 2267$ MeV/c^2, $\Gamma = 118$ MeV/c^2) which is 0.3 to 1 μb depending on the PWA solution to which the signal is added.

Figure 8 summarizes the observed yield at the DISTO energy of 2.85 GeV, the coherent upper limit from Ref. [10] at 3.5 GeV, the upper limit from the 2.5 GeV DISTO measurement, the upper limit extracted herein from the 3.5 GeV HADES data set, and the unpublished calculations of a production cross section for the $\overline{K}NN$ cluster by Akaishi, taken from Ref. [41]. Additionally, the Fäldt-Wilkin parametrization that interpolates the $\Lambda(1405)$ production cross sections (dotted line Fig. 1) is shown (scaled down by a factor of two to fit the figure boundaries). Because the production of the $\overline{K}NN$ might follow the $\Lambda(1405)$-doorway scenario, the $\Lambda(1405)$ cross section is a good starting point from which to estimate the $\overline{K}NN$ production cross section by multiplying the former by a sticking probability of a few percent [42]. While the upper limits for a visible signal strength at 2.5 and 3.5 GeV lie apparently below the unpublished calculations of Ref. [41], the DISTO value does exceed it by a factor of four, which is very surprising. More strikingly, the cross section of *X(2265)* also exceeds the $\Lambda(1405)$ production cross section, which is hardly possible in the doorway scenario. No clear explanation for the excess with respect to the other cross sections at this specific energy was made available so far, making this value incompatible with the given upper limits.

B. Qualitative observations at different $p + p$ beam kinetic energies

Besides the quantitative information discussed in the previous section there are several $p\Lambda$ invariant mass spectra that have been published in the last years. Figures 9 and 10 contain a compilation of these spectra at various beam kinetic energies. For the production of a state with mass $M = 2265$ MeV/c^2, the threshold beam kinetic energy is $E_{\mathrm{Kin}} = 2.18$ GeV. Given the large width of the signal it could also be produced at an energy of $E_{\mathrm{Kin}} = 2.16$ GeV. If the hypothesis is true that a kaonic nuclear cluster is predominantly produced via the $\Lambda(1405)$-doorway scenario [23,24], the threshold for the production of a $\overline{K}NN$ is $E_{\mathrm{Kin}} = 2.35$ GeV [respecting the low mass of the $\Lambda(1405)$ in $p + p$ collisions [27]].

The spectra collected here give only a qualitative impression of a potentially visible signal because no analyses in this respect were performed. Nevertheless, no excess of the data over the pertinent models in the region of the *X(2265)* signal (green box) is evident. It seems as if there is no hint of a strong visible signal of *X(2265)* in any of the available data sets, which means that, if a signal is present, its cross section can only be a small fraction of the total $pK^+\Lambda$ final state.

There are also other measurements at the same energy as the two DISTO data sets. Figure 11 shows the missing mass for the K^+ [44] (at 2.85 GeV, $\theta_{K^+} = 17^\circ$) and [37] (2.54 GeV, $\theta_{K^+} = 20^\circ$). The data exhibit no significant structure in the indicated *X(2265)* signal range. One has to note, however, that these are inclusive spectra of the production of a residue X_R together with a K^+. X_R can, depending on the available energy, be composed of Λp, $\Lambda N\pi$, ΣN, and $\Sigma N\pi$. While in an exclusive analysis, as done in the DISTO and HADES cases, X_R is identified with the $p\Lambda$ system, in Fig. 11 all possible decay channels of the kaonic nuclear cluster (YN and $YN\pi$) are summarized. This is, on the one hand, a disadvantage,

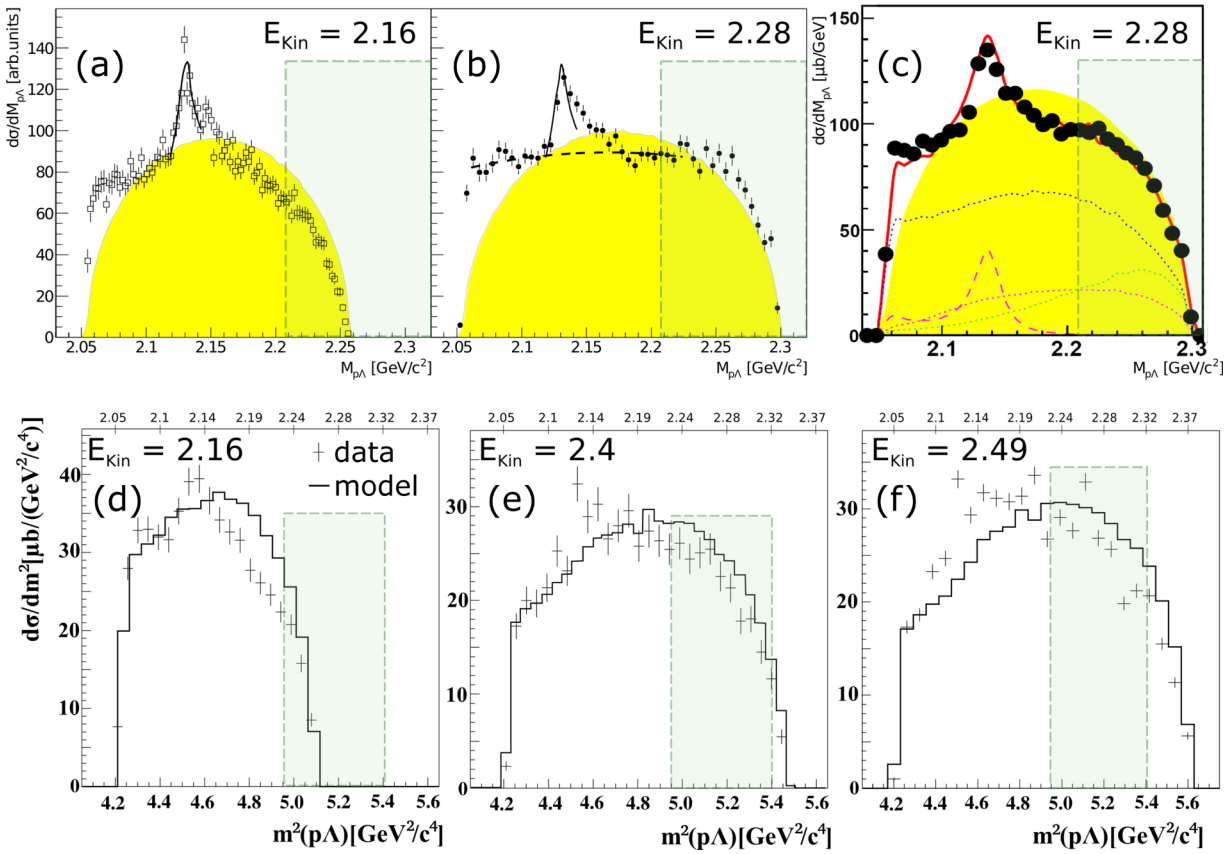

FIG. 9. (Color online) The upper row (a)–(c) shows measurements from the COSY-TOF Collaboration at two different beam kinetic energies [16]. The data are compared to phase-space simulations indicated in yellow. The lower row (d)–(f) shows also data from the COSY-TOF Collaboration at slightly higher beam kinetic energies [8]. The measured data are compared with a model that includes N^* resonances and final-state interactions. The green boxes mark the range of the *X(2265)* signal ($M \pm \Gamma/2$).

because the background description for the sum of several channels is more difficult than in an exclusive analysis. On the other hand, however, this inclusive analysis would compensate for a small branching ratio of a $\overline{K}NN$ in the $p\Lambda$ channel and a signal would thus nevertheless appear in Fig. 11, if kaonic bound states were produced with a large cross section. Under the assumption of a smooth background underneath the signal, this is obviously not the case for both data sets. Thus, also from this point of view it seems that a visible signal by a $\overline{K}NN$ cluster is not present in the data.

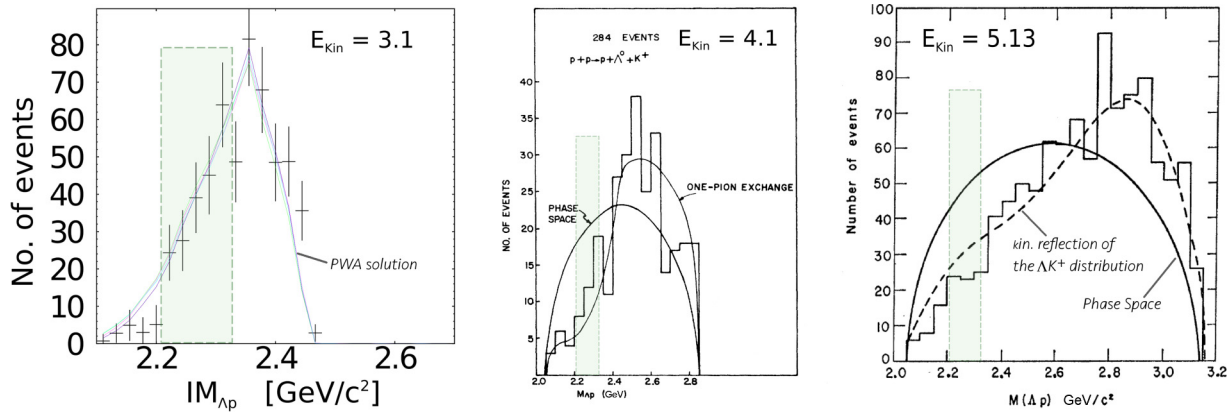

FIG. 10. (Color online) The three figures show data at a higher E_{Kin} than used for the DISTO data sets. The left figure shows data measured by FOPI [43]. They are compared to solutions from a partial wave analysis. The middle figure shows data from the Brookhaven bubble chamber [2]. The data are compared to a model of phase space and one-pion exchange. The right figure shows data from the LRL bubble-chamber experiment where the data are compared to phase-space simulations and kinematic reflections [3]. The green boxes mark the range of the *X(2265)* signal ($M \pm \Gamma/2$).

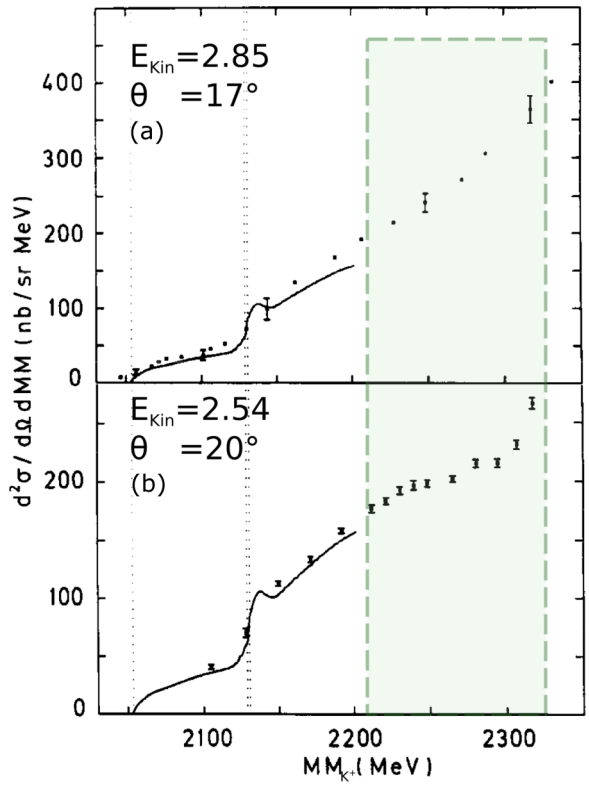

FIG. 11. (Color online) Two data sets of the missing mass to the K^+ at beam kinetic energies of 2.85 GeV, $\theta_{K^+} = 17^\circ$ (upper) and 2.54 GeV, $\theta_{K^+} = 20^\circ$ (lower) [14]. The green box marks the range of the *X(2265)* signal ($M \pm \Gamma/2$). The dashed line shows the position of the cusp structure at 2.13 GeV, which is also seen in Fig. 9.

There is one last data set at 2.83 GeV, taken by the ANKE collaboration, which contains exclusive $pK^+\Lambda$ events. Although a proposal had been set up for the analysis of the data with respect to the $\overline{K}NN$ cluster [45], it has not been pursued so far. These are probably the only data whose analysis can quickly resolve the question of whether *X(2265)* is due to a physical origin.

V. CONCLUSIONS

We summarized all available experimental measurements of $p + p$ collisions relevant for the search of the lightest kaonic nuclear bound state "ppK^-" to cross-check the hypothesis that the signal *X(2265)*, reported by the DISTO collaboration, can be associated with a kaonic nuclear bound state $\overline{K}NN$.

The signal is missing at low ($E_{\mathrm{Kin}} < 2.85$ GeV) and high ($E_{\mathrm{Kin}} > 2.85$ GeV) beam kinetic energies. Its absence cannot be explained by a depletion of the $\Lambda(1405)$ yield as was explained with help of Fig. 1. The upper limits for the production cross section of *X(2265)* set at 2.5 and 3.5 GeV suggest that its contribution to the total $pK^+\Lambda$ production cross section is only a few percent.

The strongest argument against the $\overline{K}NN$ interpretation of *X(2265)* comes from the method with which the signal was extracted. The deviation-spectrum technique to search for a new signal is not applicable if the employed model is not under firm control and if the applied cuts arbitrarily influence the outcome of the spectra.

Thus, we think that the structure *X(2265)* is very unlikely to be due to a kaonic nuclear bound state.

On the other hand, the extracted upper limits are still rather sizable and on the order of the yield predicted in Ref. [41], which leaves room to find a true signal of the kaonic nuclear bound state in $p + p$ data. This calls for new and high-statistics experiments to measure the $pK^+\Lambda$ final state, possibly also employing polarization, and their subsequent analysis with modern techniques such as a partial wave analysis [10]. The best data set so far for such an analysis is indeed that measured by DISTO with 400 000 $pK^+\Lambda$ events (2.85 GeV). Given the fact that N^* resonances do play a dominant role in the $pK^+\Lambda$ final state and given the fact that one data set is not enough to pursue a partial wave analysis with a unique solution, as shown in Ref. [10], we call for a simultaneous analysis of all available $pK^+\Lambda$ data sets to finally pin down the issue of $\overline{K}NN$ production in $p + p$ collisions.

ACKNOWLEDGMENTS

We kindly thank P. Piroue for providing us a nice version of Fig. 5, and A. Gal for the suggestions for improving the text and Fig. 8. This work was supported by the following grants: Deutsche Forschungsgemeinschaft EClust 153, Deutsche Forschungsgemeinschaft FA 898/2-1, BMBF 05P12WOGHH, and Forschungs- und Entwicklungsvertrag TMLFRG1316.

[1] R. L. Cool, T. W. Morris, R. R. Rau, A. M. Thorndike, and W. L. Whittemore, Production of *V* particles by 3-BeV protons, Phys. Rev. **108**, 1048 (1957).

[2] E. Bierman, A. Colleraine, and U. Nauenberg, Search for dibaryon resonant states, Phys. Rev. **147**, 922 (1966).

[3] W. Chinowsky *et al.*, Production of K mesons in three-body states in proton-proton interactions at 6 BeV/c, Phys. Rev. **165**, 1466 (1968).

[4] M. Firebaugh, G. Ascoli, E. Goldwasser, R. Sard, and J. Wray, Strange-particle production in 8-BeV/c proton-proton interactions, Phys. Rev. **172**, 1354 (1968).

[5] L. Baksay *et al.*, Diffraction dissociation in the reaction $p + p \to \Lambda^0 K^+ p$ at the CERN ISR, Phys. Lett. B **61**, 405 (1976).

[6] W. Cleland *et al.*, The reaction $p + p \to (\Lambda^0 + K^+)p$ at 50-GeV/c and 30-GeV/c: Partial wave analysis, deck model and double regge exchange, Nucl. Phys. B **239**, 27 (1984).

[7] S. Abd El-Samad *et al.* (COSY-TOF Collaboration), Hyperon production in the channel $p + p \to K^+\Lambda p$ near the reaction threshold, Phys. Lett. B **632**, 27 (2006).

[8] S. Abd El-Samad *et al.* (COSY-TOF Collaboration), Influence of N*-resonances on hyperon production in the channel

$p + p \to K^+\Lambda p$ at 2.95, 3.20 and 3.30 GeV/c beam momentum, Phys. Lett. B **688**, 142 (2010).
[9] M. Abdel-Bary *et al.* (COSY-TOF Collaboration), Production of Λ and Σ^0 hyperons in proton-proton collisions, Eur. Phys. J. A **46**, 27 (2010).
[10] G. Agakishiev *et al.* (HADES Collaboration), Partial wave analysis of the reaction $p(3.5\ \text{GeV}) + p \to pK^+\Lambda$ to search for the "ppK^-" bound state, Phys. Lett. B **742**, 242 (2015).
[11] A. Sibirtsev, J. Haidenbauer, H.-W. Hammer, and S. Krewald, Resonances and final state interactions in the reaction $pp \to p + K^+\Lambda$, Eur. Phys. J. A **27**, 269 (2006).
[12] A. Budzanowski *et al.* (HIRES Collaboration), High resolution study of the Λ p final state interaction in the reaction $p + p \to K^+ + (\Lambda p)$, Phys. Lett. B **687**, 31 (2010).
[13] M. Röder *et al.* (COSY-TOF Collaboration), Final-state interactions in the process $\vec{p}p \to pK^+\Lambda$, Eur. Phys. J. A **49**, 157 (2013).
[14] R. Siebert *et al.*, High resolution study of hyperon nucleon interactions by associated strangeness production in pp collisions, Nucl. Phys. A **567**, 819 (1994).
[15] A. Budzanowski *et al.* (COSY-HIRES Collaboration), Cross section of the $pp \to K^+\Sigma^+n$ reaction close to threshold, Phys. Lett. B **692**, 10 (2010).
[16] S. Abd El-Samad *et al.* (COSY-TOF Collaboration), On the ΣN cusp in the $pp \to pK^+\Lambda$ reaction, Eur. Phys. J. A **49**, 41 (2013).
[17] T. Yamazaki *et al.*, Indication of a Deeply Bound Compact K^-pp State Formed in the $pp \to p\Lambda K^+$ Reaction at 2.85 GeV, Phys. Rev. Lett. **104**, 132502 (2010).
[18] M. Maggiora *et al.* (DISTO Collaboration), DISTO data on K^-pp, Nucl. Phys. A **835**, 43 (2010).
[19] A. Tokiyasu *et al.* (LEPS Collaboration), Search for K^-pp bound state via $\gamma d \to K^+\pi^-X$ reaction at $E_\gamma = 1.5$–2.4 GeV, Phys. Lett. B **728**, 616 (2014).
[20] T. Hashimoto *et al.* (J-PARC E15 Collaboration), Search for the deeply bound K^-pp state from the semi-inclusive forward-neutron spectrum in the in-flight K^- reaction on helium-3, Prog. Theor. Exp. Phys. 061D01 (2015).
[21] Y. Ichikawa *et al.*, Observation of the "K^-pp"-like structure in the $d(\pi^+, K^+)$ reaction at 1.69 GeV/c, Prog. Theor. Exp. Phys. 021D01 (2015).
[22] A. O. Tokiyasu (LEPS Collaboration), Search for the $\overline{K}NN$ bound state at LEPS/SPring-8, PoS **Hadron2013**, 180 (2013).
[23] T. Yamazaki and Y. Akaishi, (K^-,π^-) production of nuclear $\bar{K}$ bound states in proton-rich systems via Λ^* doorways, Phys. Lett. B **535**, 70 (2002).
[24] T. Yamazaki and Y. Akaishi, The basic anti-K nuclear cluster K^-pp and its enhanced formation in the $p + p \to K^+ + X$ reaction, Phys. Rev. C **76**, 045201 (2007).
[25] P. Kienle *et al.*, Formation of the $S = -1$ resonance X(2265) in the reaction $pp \to XK^+$ at 2.50 and 2.85 GeV, Eur. Phys. J. A **48**, 183 (2012).
[26] In this view the $\Lambda(1405)$, being partially a $p\bar{K}$ bound state, forms together with a proton a $\bar{K}NN$ by final-state interaction.
[27] G. Agakishiev *et al.* (HADES Collaboration), Baryonic resonances close to the $\bar{K}$ N threshold: The case of $\Lambda(1405)$ in pp collisions, Phys. Rev. C **87**, 025201 (2013).
[28] G. Faldt and C. Wilkin, Comparison of the near threshold production of η- and K-mesons in proton proton collisions, Z. Phys. A: Hadrons Nucl. **357**, 241 (1997).
[29] I. Zychor *et al.*, Shape of the $\Lambda(1405)$ hyperon measured through its $\Sigma^0\pi^0$ decay, Phys. Lett. B **660**, 167 (2008).
[30] G. Agakishiev *et al.*, Determination of the $\Sigma(1385)^0/\Lambda(1405)$ ratio in $p + p$ collisions at 3.5 GeV, Hyperfine Interact. **210**, 45 (2012).
[31] E. Epple (HADES Collaboration), Exclusive pK Lambda production in $p + p$ reactions, PoS **BORMIO2012**, 016 (2012).
[32] L. Fabbietti *et al.* (HADES Collaboration), $pK^+\Lambda$ final state: Towards the extraction of the ppK^- contribution, Nucl. Phys. A **914**, 60 (2013).
[33] E. Epple (HADES Collaboration), New boundaries for the ppK^- production in $p + p$ collisions, EPJ Web Conf. **81**, 02005 (2014).
[34] G. Agakishiev *et al.* (HADES Collaboration), The high-acceptance dielectron spectrometer HADES, Eur. Phys. J. A **41**, 243 (2009).
[35] A. Anisovich and A. Sarantsev, Partial decay widths of baryons in the spin-momentum operator expansion method, Eur. Phys. J. A **30**, 427 (2006).
[36] A. Anisovich, V. Anisovich, E. Klempt, V. Nikonov, and A. Sarantsev, Baryon-baryon and baryon-antibaryon interaction amplitudes in the spin-momentum operator expansion method, Eur. Phys. J. A **34**, 129 (2007).
[37] W. Hogan, P. Piroue, and A. Smith, K^+-Meson production in $p - p$ collisions at 2.5–3.0 GeV, Phys. Rev. **166**, 1472 (1968).
[38] T. Junk, Confidence level computation for combining searches with small statistics, Nucl. Instrum. Methods Phys. Res., Sect. A **434**, 435 (1999).
[39] A. L. Read, Modified frequentist analysis of search results (the CL_s method), CERN-OPEN-2000-205 (2000).
[40] A. L. Read, Presentation of search results: The CL_s technique, J. Phys. G **28**, 2693 (2002).
[41] K. Suzuki *et al.* (FOPI Collaboration), Search for the kaonic nuclear state, K^-pp, in the exclusive $pp \to p\Lambda K^+$ channel, Nucl. Phys. A **827**, 312c (2009).
[42] A. Gal (private communication).
[43] R. Münzer *et al.* (FOPI and HADES Collaborations), Search for the kaonic bound state ppK^- in $pp \to pK^+\Lambda$, Hyperfine Interact. **233**, 159 (2015).
[44] J. Reed *et al.*, Production of K^+ mesons in 2.85- and 2.40-BeV $p - p$ collisions, Phys. Rev. **168**, 1495 (1968).
[45] I. Zychor, Bound kaonic nuclear states with ANKE@COSY, http://collaborations.fz-juelich.de/ikp/anke/internal_notes/Zychor_report_kbs.pdf